

NACA RM E51H02

E 51 H 02

TECH LIBRARY KAFB, NM
0143253

NACA

RESEARCH MEMORANDUM

ANALYTICAL INVESTIGATION OF RAM-JET-ENGINE PERFORMANCE IN
FLIGHT MACH NUMBER RANGE FROM 3 TO 7

By Philip J. Evans, Jr.

Lewis Flight Propulsion Laboratory
Cleveland, Ohio

SS. *Unclassified*
By *Nasa Tech Pub Announcement #101*
(OFF R AUTHORIZED TO CHANGE)

B: *25 May 56*
MADE AND *NK*

GRADE OF OFFICER MAKING CHANGE)

6 Apr 61

CLASSIFIED DOCUMENT

[Redacted]
This document contains classified information affecting the National Defense of the United States within the meaning of the Espionage Laws, Title 18, USC 793 and 794, and the transmission or the revelation of its contents in any manner to an unauthorized person is prohibited by law.
Information reported to the National Aeronautics and Space Administration by the National Advisory Committee for Aeronautics, appropriate civilian agencies, and the Department of Defense, and to United States citizens of known loyalty and discretion.

NATIONAL ADVISORY COMMITTEE FOR AERONAUTICS

WASHINGTON
October 17, 1951

319.98/13

NATIONAL ADVISORY COMMITTEE FOR AERONAUTICS

RESEARCH MEMORANDUM

ANALYTICAL INVESTIGATION OF RAM-JET-ENGINE PERFORMANCE IN

FLIGHT MACH NUMBER RANGE FROM 3 TO 7

By Philip J. Evans, Jr.

SUMMARY

An analytical investigation was made of the performance of isolated ram-jet engines in the flight Mach number range from 3 to 7. Calculations were made for two types of diffuser: a high-efficiency diffuser of unspecified form having a kinetic-energy efficiency of 0.92, and a simple normal-shock diffuser. A combustion efficiency of 100 percent and a fuel having a hydrogen-carbon ratio of 0.168 were assumed.

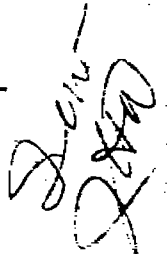
Important conclusions were: (1) a design altitude of 100,000 feet appears desirable for a high-efficiency, high Mach number ram-jet engine, and (2) gasoline provides sufficient energy release for maximum engine efficiency in the flight Mach number range investigated.

The calculated maximum propulsive-thrust coefficient for an externally mounted ram jet having a high-efficiency diffuser decreased continuously from approximately 2.13 at a flight Mach number of 3 to 0.57 at a flight Mach number of 7. The maximum engine efficiency reached a peak of 0.47 near a flight Mach number of 5 and then decreased to 0.43 at a Mach number of 7.

INTRODUCTION

Because of lack of information on ram-jet design and performance at high Mach numbers, primary consideration has been given the rocket for vehicle propulsion above a flight Mach number of 4 within the earth's atmosphere.

In order to determine whether consideration should also be given the ram jet in the high Mach number range, an analysis was made at the NACA Lewis laboratory of ram-jet performance at zero angle of attack for flight Mach numbers between 3 and 7. The computed performance was based on a hydrocarbon fuel having a hydrogen-carbon ratio of 0.168. However, because of the narrow range of hydrogen-carbon ratio and the similarity of combustion products, the same results should be obtained with most of the available hydrocarbons. In fact, it seems reasonable to expect that many nonhydrocarbons burning at the same value of energy addition will yield approximately the same thrust and engine efficiency. Consequently, results are presented in terms of an energy-addition parameter so that they will be more generally applicable.



In the analysis, two types of diffuser were considered: (1) a diffuser of unspecified form having a kinetic-energy efficiency of 0.92, and (2) a simple normal-shock diffuser, which provided a basis for comparison. The results presented are for the design condition only and represent a different geometry for each value of energy addition and flight Mach number. Off-design performance was not considered in the analysis.

SYMBOLS

The following symbols are used in this report:

- A cross-sectional area
- $C_{D,e}$ total engine-drag coefficient, $D_e/A_0 q_0$
- $C_{D,f}$ engine friction-drag coefficient, $D_f/A_0 q_0$
- C_F propulsive-thrust coefficient, $F/A_0 q_0$
- $C_{F,n}$ net-thrust coefficient, $F_n/A_0 q_0$
- C_f skin-friction coefficient, (friction force/sq ft)/ q_0
- c speed of sound, (ft/sec)
- D drag of airplane minus drag of engine
- D_e total engine drag
- D_f engine friction drag
- E_r energy-addition parameter defined as ratio between fuel energy actually added and energy added by gasoline at its stoichiometric condition
- F propulsive thrust, $F_n - D_e$
- F_n net, or internal, thrust
- f/a fuel-air ratio
- g gravitational constant, $32.17(\text{ft}/\text{sec}^2)$
- H total, or reservoir, enthalpy
- h static enthalpy

J	mechanical equivalent of heat, 778(ft-lb/Btu)
L	lift of airplane
m	mass flow
M	Mach number
P	reservoir, or total, pressure
P_r	relative total pressure as used in air tables of reference 6 (actual total pressure divided by total pressure at reference temperature used in table)
p	static pressure
p_r	relative static pressure as used in air tables of reference 6
Q	heating value of fuel, (Btu/lb fuel)
q	dynamic pressure, $\rho V^2/2$
R	gas constant in characteristic equation of state
T	reservoir, or total, temperature
t	static temperature
V	velocity
W_0	gross weight at beginning of flight
W_1	gross weight after fuel has been burned
w_f	actual fuel flow, (lb/sec)
X	range, (ft)
γ	ratio of specific heats
η_c	combustion efficiency
η_e	engine efficiency, $\frac{FV_0}{QJw_f}$
η_k	kinetic-energy efficiency of diffuser (equation (1))
η'_k	efficiency parameter for complete engine (defined by equation (3))

- ρ density
- τ total temperature after combustion divided by total temperature before combustion

Subscripts:

- av average
- comp completely expanded
- g gasoline
- eff effective
- st stoichiometric
- 0 free-stream conditions, or inlet free-stream tube
- 2 combustor inlet
- 3 downstream of flame holder
- 6 nozzle throat
- 7 nozzle exit

2258

ASSUMPTIONS AND CALCULATIONS

General Assumptions and Procedure

The following general assumptions were made:

1. The internal flow is one-dimensional. In applying the one-dimensional-flow equations, the variations in γ , the ratio of specific heats of the working fluid, due to temperature and fuel-air ratio variations were considered. For the flow inside the combustor, an average γ before and after combustion was used. The flow from the nozzle throat to the nozzle exit was calculated as described in appendix A.

2. The engine is operating at an altitude of 100,000 feet. This assumption determines the free-stream static temperature and pressure (table III of reference 1) and hence the total temperature and total-temperature ratio τ corresponding to a given flight Mach number M_0 and energy addition. It also determines the Reynolds number per unit length used to determine the external friction-drag coefficient.

3. The energy lost by radiation and conduction is negligible.
4. The free-stream area of the air entering the engine is equal to the inlet area of the engine.
5. Structural integrity is maintainable at the high temperatures and pressures.

Diffusers

Definition and significance of kinetic-energy efficiency. - The kinetic-energy efficiency η_k of a diffuser is defined as the kinetic energy the air would have after being expanded isentropically from the diffuser exit to the ambient static pressure divided by the free-stream kinetic energy. When this process is accomplished at constant γ , the formula for the kinetic-energy efficiency is

$$\eta_k = 1 - \frac{\left(\frac{P_0}{P_2}\right)^{\frac{\gamma-1}{\gamma}} - 1}{\frac{\gamma-1}{2} M_0^2} \quad (1)$$

Consequently the assumption of a value for η_k determines the diffuser total-pressure ratio P_2/P_0 for each M_0 . Equation (1) is plotted in figure 1. In this figure the total-pressure ratio required for a given value of η_k decreases rapidly with increasing flight Mach number M_0 . In the range of M_0 considered, very little error is introduced for high values of η_k by considering γ constant and equal to 1.4 since, in general, equation (1) yields accurate results whenever the final γ after reexpansion is little different from the ambient static γ .

The kinetic-energy efficiency of a diffuser is significant for ram-jet engines because of its similarity to a basic ram-jet performance parameter. The net internal-thrust coefficient of an engine having constant γ and a completely expanded exit is given by

$$\frac{1}{2} C_{F,n} = (1 + f/a) \sqrt{\tau \eta'_k} - 1 \quad (2)$$

where

$$\eta'_k = 1 - \frac{\left(\frac{P_0}{P_7}\right)^{\frac{\gamma-1}{\gamma}} - 1}{\frac{\gamma-1}{2} M_0^2} \quad (3)$$

(See appendix B for derivation of equations (2) and (3).) The quantity $\tau\eta'_k$ represents the kinetic-energy efficiency of the complete engine. Because at high values of M_0 almost all the total-pressure losses occur in the diffuser, the diffuser kinetic-energy efficiency and η'_k are nearly equal.

The shape of the curves of figure 1 (that is, the well-defined shoulder at high values of M_0) suggests that there will be little advantage in operating at total-pressure ratios very far to the right of this shoulder.

High-efficiency diffuser. - On the basis of available high Mach number data, the high-efficiency diffuser was assumed to have a kinetic-energy efficiency η_k of 0.92 at all flight Mach numbers. An advantage of assuming η_k is that knowledge of the exact form of the high-efficiency diffuser is unnecessary. The assumption that the maximum η_k is invariant with M_0 was suggested by the small variation of maximum η_k in the range of M_0 between 2 and 4 and also by the fact that there is no excessive variation of the η_k of the flow through a normal-shock wave in the M_0 range from 4 to 7. Values of η_k for several existing and proposed diffuser designs (references 2 and 3) are shown in figure 1. The value of P_2/P_0 which follows from the assumption of η_k decreases quite rapidly as M_0 increases (fig. 2) and should be attainable with a refined diffuser design.

Normal-shock diffuser. - In calculating the total-pressure ratio across the shock wave of the normal-shock diffuser, imperfect-gas effects were included by means of correction factors taken from reference 4. The total-pressure ratio of the subsonic diffuser was arbitrarily assumed to be 0.98. The resultant over-all total-pressure ratio of the normal-shock diffuser is considerably lower than that of the high-efficiency diffuser; however, its variation with M_0 is quite similar (fig. 2).

Combustion

Assumptions pertaining to the combustion process were made as follows:

1. The fuel is any hydrocarbon (such as gasoline) having a hydrogen-carbon ratio of 0.168. However, because of the similarity of combustion products of hydrocarbons, the resulting total-temperature ratio τ across the combustor at equal values of energy addition (based on data from reference 5) should be very nearly equal for all

hydrocarbons; and even for some nonhydrocarbons being considered for ram-jet fuels, a given energy addition should produce at least approximately the same value of τ . Consequently, the resulting thrust coefficients and engine efficiencies will apply to most hydrocarbon fuels and to a few nonhydrocarbons as well. Thus, instead of presenting performance in terms of fuel-air ratio, as is frequently done, it is presented in terms of an energy-addition parameter E_r defined as

$$E_r = \frac{(f/a)_{\text{eff}} Q}{(f/a)_{g, \text{st}} Q_g}$$

If the fuel is gasoline, E_r is merely the effective fuel-air ratio relative to stoichiometric, that is, the equivalence ratio. For other fuels, however, this energy-addition parameter E_r is the ratio between the energy actually added and the energy that would be added by gasoline at its stoichiometric condition.

2. In the determination of τ it is necessary that the value of combustor-inlet pressure p_2 be consistent with the assumed altitude and diffuser-pressure ratio, because the amount of molecular dissociation increases as the pressure decreases, causing the resultant τ to decrease. The difference in the pressure given by the two types of diffuser at high values of M_0 (noticeable from fig. 2) results in two sets of curves of τ against M_0 for constant value of energy-addition parameter (fig. 3). The large decrease of τ with increasing M_0 is mainly a result of the increase of total temperature with M_0 .

3. Combustion is completed in the constant-area combustor.

4. The total-pressure drop across the flame holder is equal to twice the dynamic pressure ahead of the flame holder, that is

$$P_2 - P_3 = 2q_2 = \rho_2 V_2^2$$

This value is probably somewhat high at large values of M_0 because the high temperatures encountered should permit the use of a low-loss flame holder, but the resulting difference in thrust is small at the value of combustor-inlet Mach number assumed herein.

5. The design value of the combustor-inlet Mach number M_2 was taken as 0.15. For the range of M_0 investigated, this value of M_2 is so low that there is no choking in a straight pipe at the lower values of M_0 , and hence no limitation on τ imposed from this source. Some calculations were also made for $M_2 = 0.05$ to check the effect of this variable on the engine geometry.

In order to provide background on combustion requirements, it seemed advisable to include the range of combustor-inlet conditions (p_2 , T_2 , and V_2) encountered (fig. 4).

The combustor-inlet pressure p_2 (fig. 4(a)) corresponds to $M_2 = 0.15$; at such low values of M_2 , however, p_2 changes very little with M_2 . At high flight Mach numbers and altitudes much below 100,000 feet, the high-efficiency engine may have serious structural difficulties because of the combination of high temperature and pressure encountered. Because the p_2 of the normal-shock engine is much lower, the structural difficulties are considerably lessened; but at high altitudes, p_2 may be low enough to cause combustion difficulties.

The total temperature of the inlet air T_2 that was used herein was determined from the air tables of reference 6 (see appendix A). In order to show that some refinement is necessary, the exact value from the air tables is compared with the value obtained by assuming constant γ equal to 1.4 (fig. 4(b)). At $M_0 = 7$, the error is 470° R. These values of total temperature apply to the isothermal region of the atmosphere between altitudes of 35,000 and 105,000 feet. Above an altitude of 105,000 feet, performance is reduced because the increased ambient air temperature results in a reduced total-temperature ratio across the combustor. Since altitudes below 100,000 feet may be undesirable because of the high pressure, a reasonable compromise seems to be an altitude of 100,000 feet for design of high-efficiency, high Mach number ram-jet engines. This altitude was therefore chosen for the analysis.

Although the values of V_2 (fig. 4(c)) may seem high for $M_2 = 0.15$, they are not unreasonable and fall within the range currently used in afterburners.

External Drag

The external drag was computed for a surface that is uniformly tapered from the inlet to the exit. The linearized supersonic-flow data of reference 7 were used to estimate the wave drag. The wave drag above $M_0 = 4$ was obtained by extrapolation from reference 7 according to the linearized supersonic-flow similarity rule.

For some engines the contour may be curved, or it may consist of broken straight lines; the error is small, however, because the wave drag is only a small part of the total drag and the total drag is small compared with the propulsive thrust.

Friction drag. - A turbulent flat-plate boundary layer was assumed over the entire outer surface. Because there is a possibility that a portion of the boundary layer may be laminar, the drag used herein is near the maximum possible. An effective engine length of 20 feet and an altitude of 100,000 feet were used to determine the skin-friction coefficient.

The skin-friction coefficient (fig. 5) was determined by using reference 8 and an unpublished report of Morris W. Rubesin of the Ames laboratory. The coefficient used is from 10 to 20 percent higher than the extended Frankl and Voishel value of reference 9, which is shown therein to agree closely with the available experimental data. However, because the experimental data were all near $M_0 = 2$ and 2.5, the accuracy of the skin friction used at higher values of M_0 is yet to be determined. In any event, the engine drag is small compared with the propulsive thrust and errors due to lack of knowledge of drag at the high Mach numbers are not expected to change appreciably the results obtained.

Total drag. - The total drag, consisting of the friction drag plus the wave drag, was calculated over a range of over-all area ratio A_0/A_7 (fig. 6). The values used were for a fineness ratio (length divided by mean diameter) of 8. This value was selected because it is a reasonable value for a ram jet. It is clear that in the A_0/A_7 range of this analysis, the principal portion of the drag is friction drag.

Nozzle

The main assumption pertaining to the nozzle concerns the method of accounting for the imperfect-gas effects as discussed in appendix A. The assumed nozzle total-pressure ratio P_7/P_6 between the throat and the exit was 0.96 for all amounts of expansion.

Nozzle expansion corresponding to maximum thrust. - The maximum internal thrust occurs for the completely expanded exit ($p_7 = p_0$) if the nozzle losses do not vary with the amount of expansion, as was assumed herein. However, for the high-efficiency engine the resultant propulsive thrust is maximum when the nozzle is slightly underexpanded, that is, when p_7 is somewhat greater than p_0 , because when p_7 is near p_0 the external drag increases more rapidly than the internal (net) thrust as the amount of expansion is increased. In order to find the maximum propulsive thrust and the corresponding amount of expansion, it is necessary to investigate net thrust and drag over a range of p_7/p_0 . The calculations show that there is little difference between the maximum propulsive thrust and the propulsive thrust of the completely expanded nozzle and that there is a fairly large range of p_7/p_0 over which the propulsive thrust is almost constant. Typical variations of C_F and $C_{F,n}$ with p_7/p_0 are presented in figure 7. These curves are for the energy-addition parameter E_r equal to 0.4 and hence do not necessarily correspond to the condition of maximum engine efficiency. Similar curves (not shown) were plotted for other values of E_r for the high-efficiency engine in order to obtain the value and location of the

maximums. The values of p_7/p_0 corresponding to the maximum thrusts obtainable at the value of E_r corresponding to maximum engine efficiency are shown in figure 8 for the high-efficiency engine. The amount of expansion is also presented in terms of the exit area A_7 corresponding to maximum thrust divided by the exit area corresponding to complete expansion $A_{7,comp}$. On this basis the expansion corresponding to maximum thrust becomes considerably less than complete at the higher values of M_0 . This optimum amount of expansion must vary appreciably with the assumed external drag because if there were no external drag, complete expansion would be optimum.

RESULTS AND DISCUSSION

Propulsive-Thrust Coefficient and Engine Efficiency

The performance of the high-efficiency engine for various values of the flight Mach number M_0 is shown in figure 9 in terms of the ratio of engine efficiency to combustion efficiency η_e/η_c as a function of propulsive-thrust coefficient C_F . The maximum values of propulsive-thrust coefficient and η_e/η_c are plotted in figures 10 and 11, respectively. The maximum propulsive-thrust coefficient (at $E_r = 1.0$, which is stoichiometric for gasoline) decreases continuously from 2.13 at $M_0 = 3$ to 0.57 at $M_0 = 7$ (fig. 9 or 10). The rapid decrease of the propulsive-thrust coefficient with increasing M_0 is mainly a result of the decrease of total-temperature ratio τ . More thrust could be obtained by the use of a fuel having a higher energy release than gasoline (that is, $E_r > 1.0$), but such an increase in thrust would be accompanied by a decrease in engine efficiency.

The engine efficiency reaches its maximum value of approximately 0.47 near $M_0 = 5$ and then decreases gradually to approximately 0.43 at $M_0 = 7$. As can be seen from the Breguet range formula

$$X = QJ\eta_e \frac{L}{D} \log_e \frac{W_0}{W_1}$$

the range is proportional to η_e and hence the high value of η_e that may be attainable at the large values of M_0 will be an important factor in the consideration of long-range, high-speed ram-jet-propelled vehicles.

As the energy-addition parameter E_r increases (fig. 9), C_F increases and η_e/η_c increases to a maximum and then decreases. The value of E_r corresponding to the maximum η_e/η_c increases

with M_0 from approximately 0.35 at $M_0 = 3$ to 0.8 at $M_0 = 7$. This trend indicates that slightly above $M_0 = 7$ gasoline may no longer have sufficient energy release for maximum possible engine efficiency. In this event a fuel permitting greater energy addition than gasoline should be used. However, since at η_c near 100 percent gasoline does have sufficiently high energy release in the Mach number range of interest, the use of fuels permitting a higher energy release may not be necessary for the attainment of maximum efficiency. Other fuel characteristics are important; the range is proportional to the heating value per pound of the fuel as well as to the engine efficiency, and the density of the fuel is of great importance in any flight vehicle design. Such considerations, however, are outside the scope of this investigation.

A comparison of the propulsive-thrust coefficients and the engine efficiencies of both the high-efficiency and the normal-shock engines is made in figures 10 and 11, respectively. The maximum propulsive-thrust coefficient of the normal-shock engine is near 1.57 at $M_0 = 3$, about three-fourths that of the high-efficiency engine, and approximately zero at $M_0 = 7$ (fig. 10).

The maximum engine efficiency of the normal-shock engine (about 0.27) is only 57 percent of that of the high-efficiency engine and occurs at a lower flight Mach number ($M_0 = 4$) (fig. 11).

Area and Volume Relations

It follows from the one-dimensional compressible-flow equations that for any given combustor-inlet Mach number M_2 there exists a value of M_0 above which the inlet flow area A_0 is greater than the combustor flow area A_2 . The values of M_0 above which the inlet area of the high-efficiency diffuser becomes greater than combustor area are 5.7 for $M_2 = 0.05$, 3.6 for $M_2 = 0.15$, and about 2.9 for $M_2 = 0.25$. For the normal-shock diffuser, unless the design M_2 is extremely high (approximately 0.42 at all values of M_0), the combustor area is greater than the inlet area. The significance of this condition of equal areas is that it is close to the condition where the combustor starts interfering with the external contour; it is not especially critical, however, because the combustor area must be somewhat greater than the inlet area before interference starts owing to the taper of the external contour, and also because there can be a small amount of interference before the drag is increased appreciably. A qualitative picture of this situation is given in figure 12, which presents sketches of engines with areas in correct proportion for various values of M_0 and M_2 . It can be seen that engines designed for maximum engine efficiency have approximately the same A_0/A_7 for all values of M_0 considered. Of interest is the

fact that for a given amount of expansion, variations in M_2 have little effect on the value of A_0/A_7 . Only one sketch of the normal-shock engine (fig. 12(a)) is shown because there are no significant variations of appearance with M_0 . The following discussion will therefore pertain to the high-efficiency engine only (figs. 12(b), 12(c), and 12(d)). The spike diffuser shown in the sketches is purely schematic and is not intended to imply the diffuser design.

At $M_0 = 3$, low values of M_2 of the order of 0.05 will result in undesirable external drag increases, whereas for $M_2 = 0.15$ the combustor interferes only slightly with the assumed external contour. At $M_0 = 5$ and $M_2 = 0.05$, the combustor still interferes slightly; whereas at $M_2 = 0.15$ there is no interference at all. At $M_0 = 7$, M_2 can be made even smaller than 0.05 before the external contour will be affected. Figure 12 also illustrates how much the usable volume increases with M_0 and M_2 . This increased volume may be a reason for selecting a value of M_2 as high as good combustion permits.

CONCLUDING REMARKS

An analytical investigation was made of the performance of an externally mounted ram-jet engine in the flight Mach number range from 3 to 7 with diffusers of two types, one of undetermined form with a kinetic-energy efficiency of 0.92, and the other, a simple normal-shock diffuser. A combustion efficiency of 100 percent and a fuel having a hydrogen-carbon ratio of 0.168 were assumed. The results obtained were:

1. A design altitude of about 100,000 feet appears desirable for a high-efficiency high Mach number ram-jet engine in order to avoid the excessive pressures encountered at lower altitudes and the increased ambient temperatures encountered at higher altitudes.
2. Gasoline provides sufficient energy release for maximum engine efficiency in the flight Mach number range investigated. At Mach numbers above 7 and for vehicle designs requiring maximum thrust even at the expense of efficiency, however, fuels permitting higher energy release are indicated.
3. For the high-efficiency engine the maximum propulsive-thrust coefficient decreased continuously from 2.13 at a flight Mach number of 3 to 0.57 at a flight Mach number of 7; whereas, for the normal-shock engine, this same coefficient decreased from 1.57 to zero in the same Mach number range. The maximum engine efficiency of the

high-efficiency engine increased to a maximum of 0.47 near a flight Mach number of 5 and then decreased gradually to about 0.43 at a Mach number of 7; whereas, the maximum for the normal-shock engine was only 0.27 and occurred near a Mach number of 4.

Lewis Flight Propulsion Laboratory
National Advisory Committee for Aeronautics
Cleveland, Ohio

APPENDIX A

PROBLEMS ASSOCIATED WITH VARIATIONS IN γ

Since at high flight Mach numbers M_0 large variations of temperature, and hence large variations in the ratio of specific heats γ , are unavoidable, the usual formulas and tables for constant γ are no longer strictly applicable. In order to obtain the total temperature when given M_0 and the ambient static temperature t_0 , use is made of the air table (reference 6) and the energy equation

$$H_0 = h_0 + \frac{M_0^2 c_0^2}{2gJ}$$

The ambient static enthalpy h_0 and the ambient speed of sound c_0 depend on t_0 only, and hence the total enthalpy H_0 is readily calculated; then the corresponding value of total temperature can be obtained from the air table. The corresponding ratio of static to total pressure can be easily found because it equals the relative-pressure ratio $p_{r,0}/P_{r,0}$, where p_r and P_r are tabulated with the static and total temperatures, respectively, in the air table.

Although it would have been desirable, such a procedure was not possible for exhaust-nozzle calculations because of the lack of corresponding tables for combustion products at the high temperatures encountered. Therefore, in order to calculate exit conditions, a constant value of γ was used equal to

$$\gamma_{av} = \frac{\gamma_{a,7} + \gamma_7}{2}$$

where $\gamma_{a,7}$ corresponds to the total temperature after combustion and γ_7 was determined from the static exit temperature t_7 . Since t_7 depends on γ_{av} , an iteration procedure had to be used. It converged very rapidly, however. This method permits the calculation of the temperature ratio t_7/T_7 and hence M_7 when p_7/P_7 is known. The area ratio A_0/A_7 can then be calculated from the usual one-dimensional energy and mass-flow considerations.

It is very important to use the proper form of the thrust equation, namely,

$$\frac{1}{2} C_{F,n} = (1 + f/a) \frac{M_7}{M_0} \sqrt{\frac{\gamma_7 R_7 t_7}{\gamma_0 R_0 t_0}} - 1 + \frac{\frac{p_7}{p_0} - 1}{\gamma_0 M_0^2 \frac{A_0}{A_7}} \quad (A1)$$

instead of

$$\frac{1}{2} C_{F,n} = \frac{\frac{p_7}{p_0} (\gamma_7 M_7^2 + 1) - (\gamma_0 M_0^2 \frac{A_0}{A_7} + 1)}{\gamma_0 M_0^2 \frac{A_0}{A_7}} \quad (A2)$$

Equation (A1) follows directly from equation (B2) (see appendix B) because

$$V = M \sqrt{\gamma R t}$$

Equation (A2) follows most easily from equation (B1) because

$$mV = \rho AV^2 = \gamma p M^2 A$$

Equations (A1) and (A2) are equivalent and would both yield the same answer if the correct value of A_0/A_7 were used. However, equation (A2) is very sensitive to errors in A_0/A_7 . Equation (A2) can be used to advantage in calculating A_0/A_7 once $C_{F,n}$ has been found from equation (A1) because then the situation is reversed and A_0/A_7 will be insensitive to $C_{F,n}$. An iteration procedure for calculating A_0/A_7 is suggested; namely, use of a very approximate value for A_0/A_7 in equation (A1) and then use of the resulting value of $C_{F,n}$ in equation (A2) to obtain a more accurate value of A_0/A_7 . Such a procedure works very well for nozzles in the range of expansion encountered.

APPENDIX B

DERIVATION OF THRUST EQUATIONS

From the equation for the net (internal) thrust

$$F_n = m_7 V_7 - m_0 V_0 + (p_7 - p_0) A_7 \quad (B1)$$

the net-thrust coefficient is found to be

$$C_{F,n} = 2 \left(\frac{m_7 V_7}{m_0 V_0} - 1 \right) + \frac{p_7 - p_0}{\frac{1}{2} \gamma_0 p_0 M_0^2 \frac{A_0}{A_7}} \quad (B2)$$

Equation (2) can be derived from equation (B2) in the following manner:

From the energy equation, the velocity ratio can be expressed as

$$\frac{V_7^2}{V_0^2} = \frac{H_7 - h_7}{H_0 - h_0}$$

which becomes, for constant γ ,

$$\frac{V_7^2}{V_0^2} = \frac{T_7 - t_7}{T_0 - t_0} = \frac{\frac{T_7}{T_0} \left(\frac{T_0}{t_0} - 1 - \frac{t_7/T_7}{t_0/T_0} + 1 \right)}{\frac{T_0}{t_0} - 1} \quad (B3)$$

By use of the definition of τ , the energy relation between temperature and Mach number, the isentropic relation between temperature and pressure, and the definition of η'_k given by equation (3), equation (B3) can be reduced to

$$\frac{V_7^2}{V_0^2} = \tau \eta'_k \quad (B4)$$

when $p_7 = p_0$. Hence, since $\frac{m_7}{m_0} = 1 + f/a$, equation (2) follows from equations (B2) and (B4).

REFERENCES

1. Warfield, Calvin N.: Tentative Tables for the Properties of the Upper Atmosphere. NACA TN 1200, 1947.
2. Ferri, Antonio, and Nucci, Louis M.: Theoretical and Experimental Analysis of Low-Drag Supersonic Inlets Having a Circular Cross Section and a Central Body at Mach Numbers of 3.30, 2.75, and 2.45. NACA RM L8H13, 1948.
3. Dankhoff, W. F.: A Performance Analysis of the Hermes B-1 Supersonic Ramjet. Rep. No. 55267, Thermal Power Systems Div., Gen. Elec. Co., Aug. 1948. (Project Hermes, U.S. Army Ordnance.)
4. Meyerhoff, Leonard, and Reissner, Hans J.: The Standing, One-Dimensional Shock Wave Under the Influence of Temperature-Dependent Viscosity, Heat Conduction and Specific Heat. PIBAL Rep. No. 150, Aero. Eng. and Appl. Mech. Dept., Polytechnic Inst. of Brooklyn, June 1949. (Contract No. N6onr-206, Task Order 1.)
5. McCann, W. J.: Thermodynamic Charts for Internal-Combustion-Engine Fluids. NACA TN 1883, 1949. (Revised by L. R. Turner and Emory A. Bauer.)
6. Keenan, Joseph H., and Kaye, Joseph: Thermodynamic Properties of Air. John Wiley & Sons, Inc., 1945.
7. Jack, John R.: Theoretical Wave Drags and Pressure Distributions for Axially Symmetric Open-Nose Bodies. NACA TN 2115, 1950.
8. Schlichting, H.: Lecture Series "Boundary Layer Theory." Part II - Turbulent Flows. NACA TM 1218, 1949.
9. Rubesin, Morris W., Maydew, Randall C., and Varga, Steven A.: An Analytical and Experimental Investigation of the Skin Friction of the Turbulent Boundary Layer on a Flat Plate at Supersonic Speeds. NACA TN 2305, 1951.

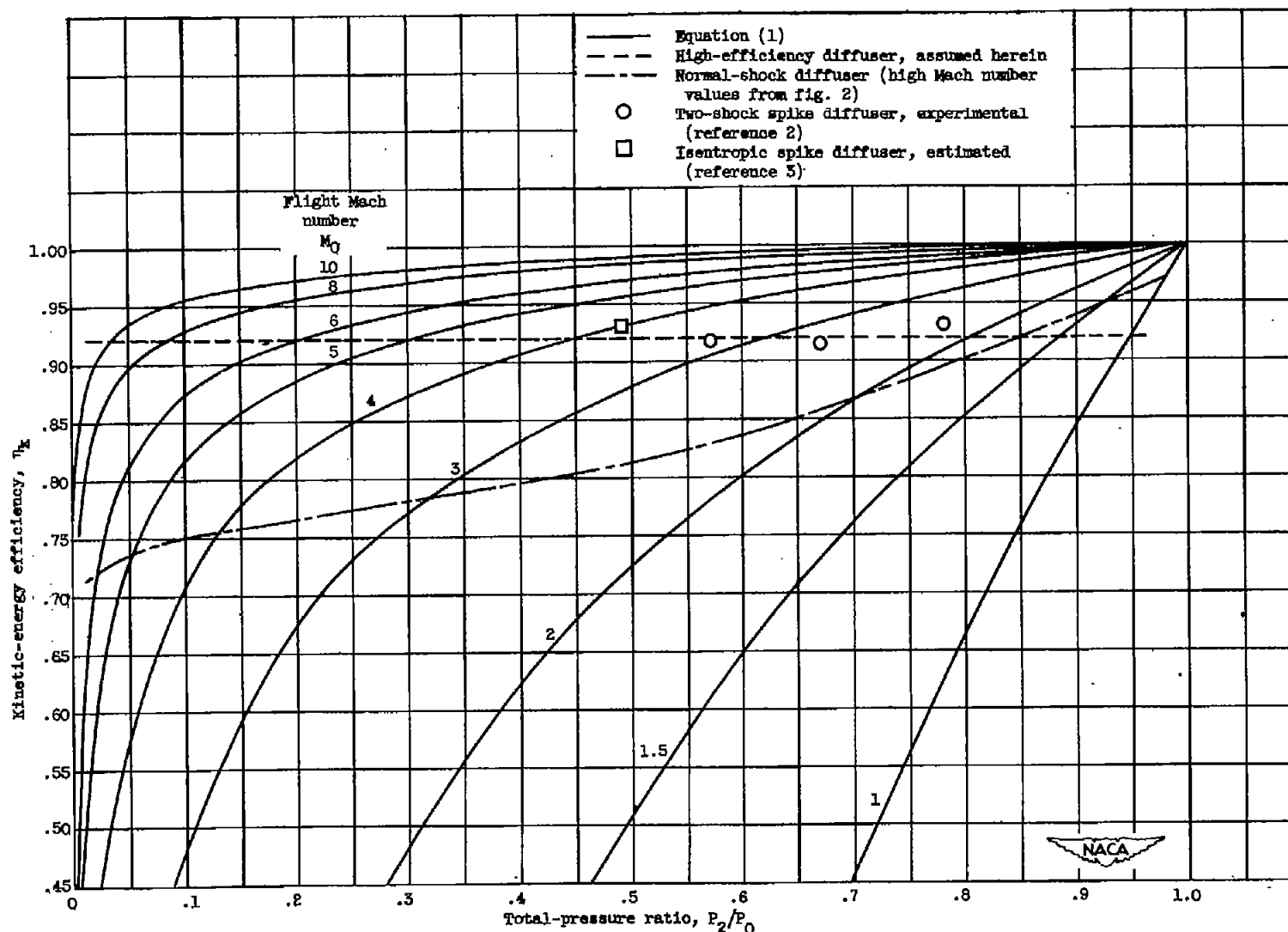


Figure 1. - Variation of kinetic-energy efficiency with total-pressure ratio for several values of flight Mach number, including values assumed herein, as well as values for several specific diffuser designs.

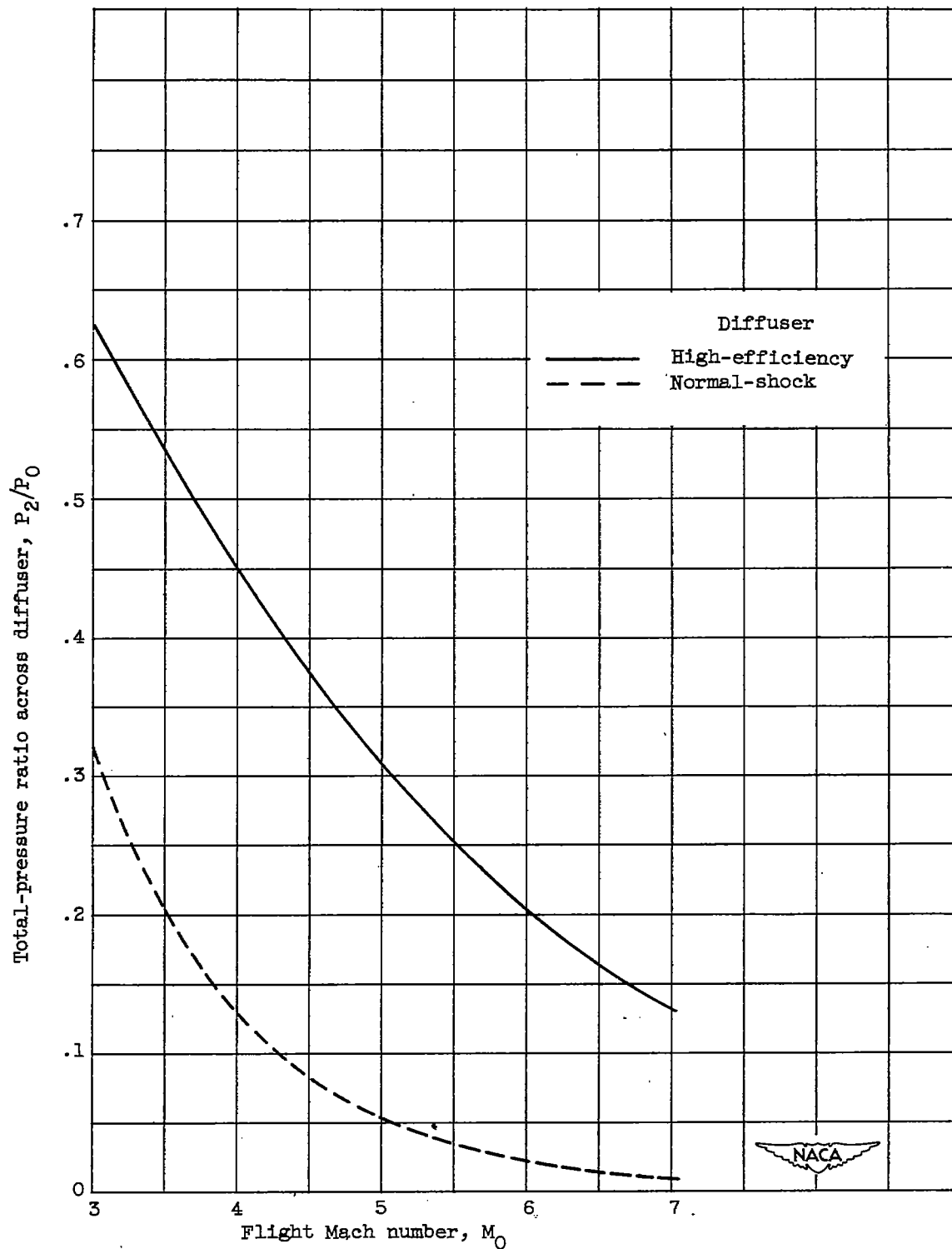


Figure 2. - Variation of total-pressure ratio across diffuser with flight Mach number.

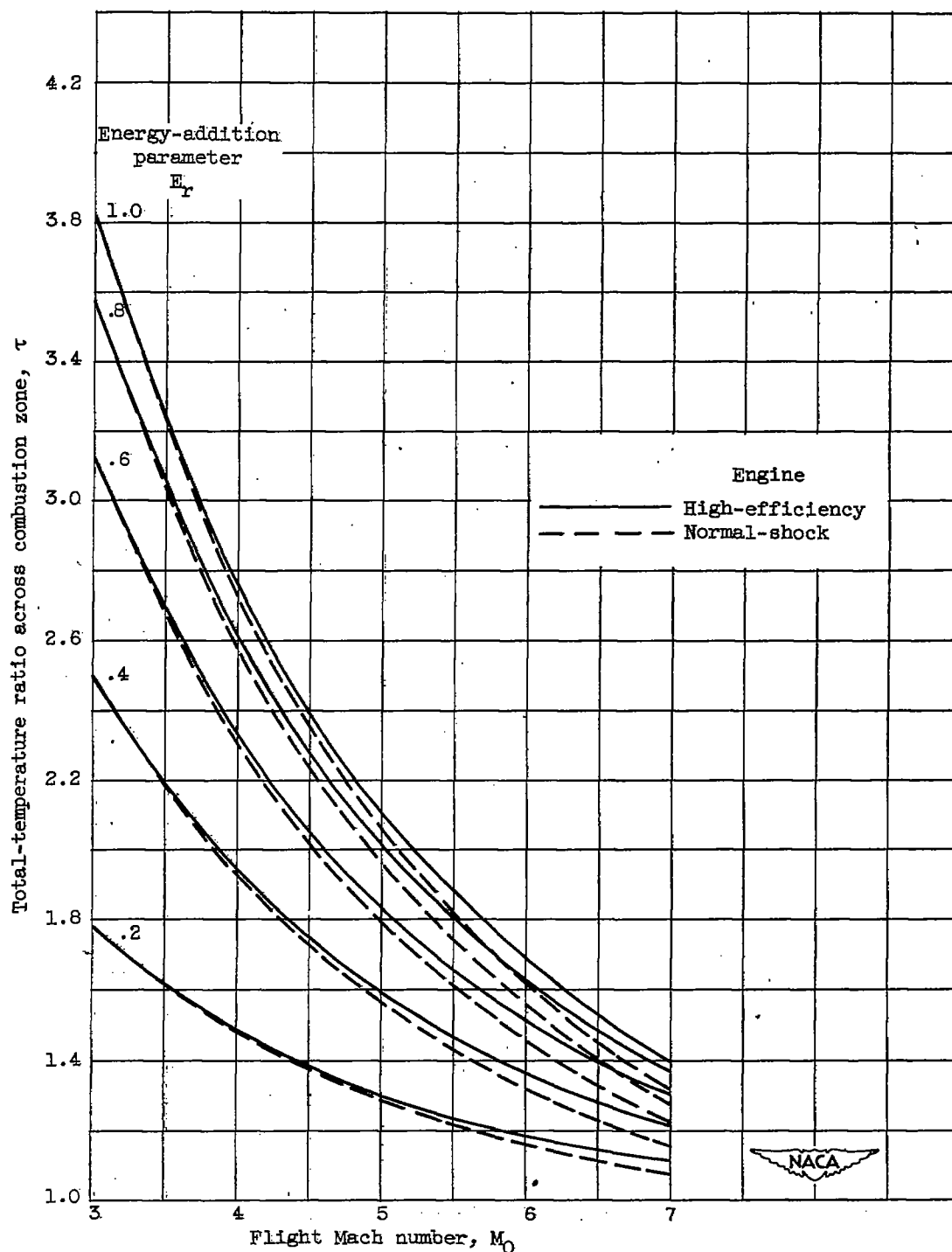
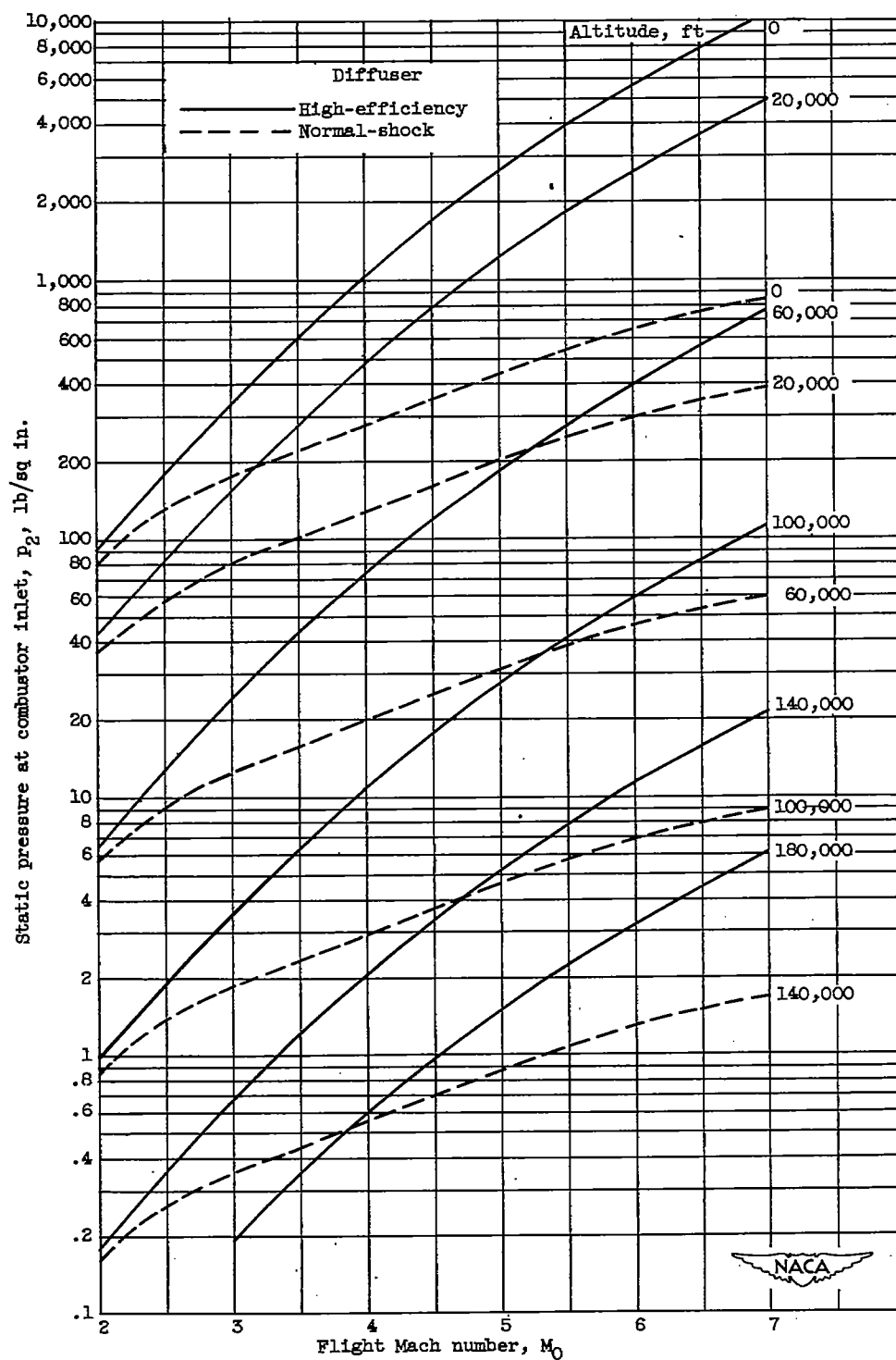


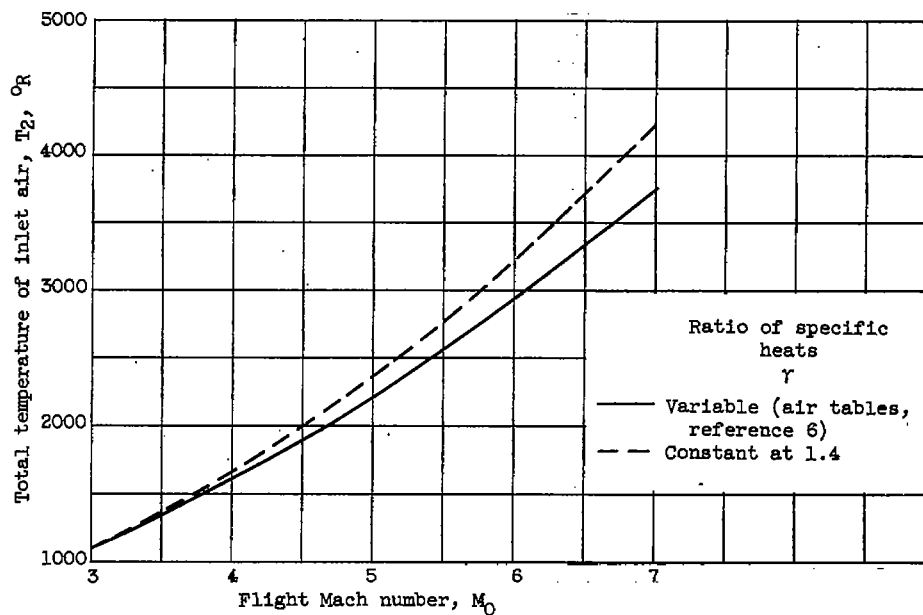
Figure 3. - Variation of total-temperature ratio across combustion zone with flight Mach number for several values of energy-addition parameter for both high-efficiency and normal-shock engines. Hydrocarbon fuel; altitude, 100,000 feet.



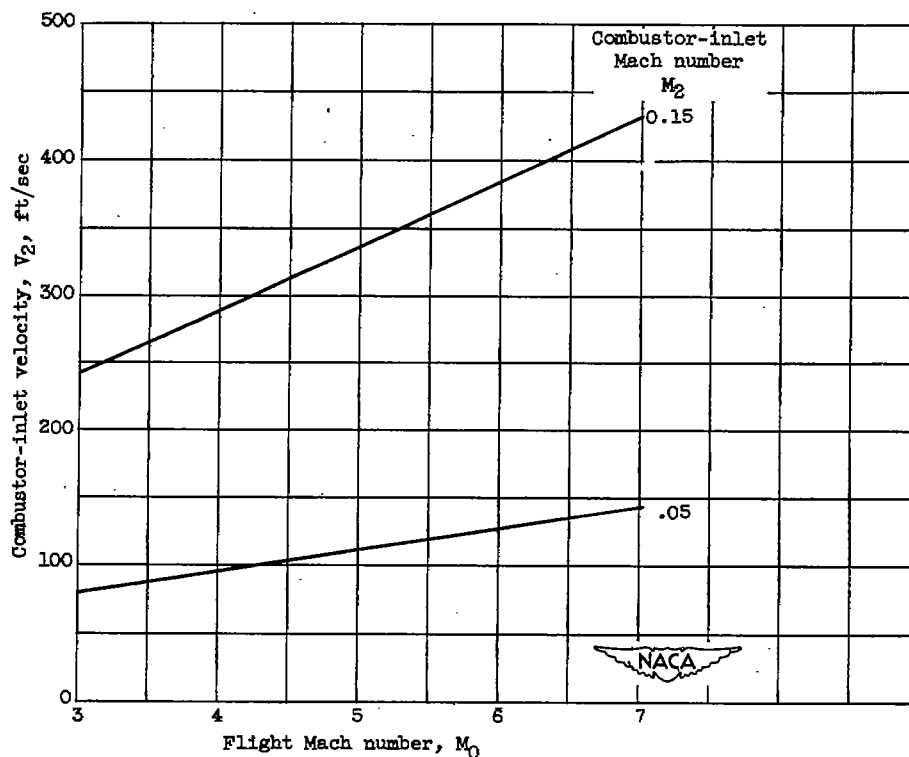
(a) Static pressure at combustor inlet for various altitudes.
High-efficiency and normal-shock diffusers.

Figure 4. - Variation of combustor-inlet conditions with flight Mach number.

CONFIDENTIAL



(b) Total temperature of inlet air for two methods of computation.
Ambient static temperature, 392°R .



(c) Velocity at combustor inlet for various values of combustor-inlet Mach number. Speed of sound based on temperature obtained from air tables. Ambient static temperature, 392°R .

Figure 4. - Concluded. Variation of combustor-inlet conditions with flight

CONFIDENTIAL

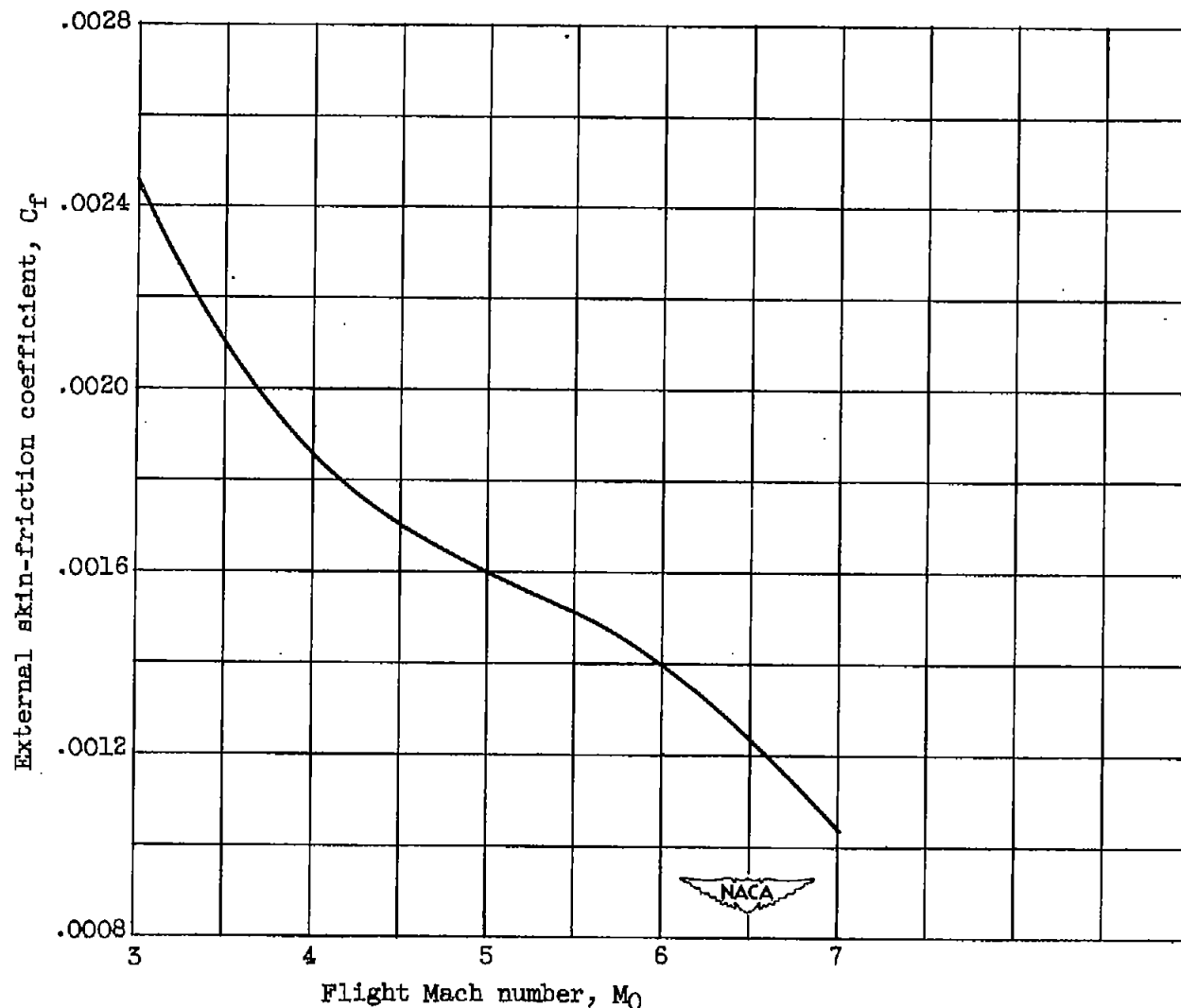


Figure 5. - Variation of external skin-friction coefficient with flight Mach number. Turbulent boundary layer; effective engine length, 20 feet; altitude, 100,000 feet.

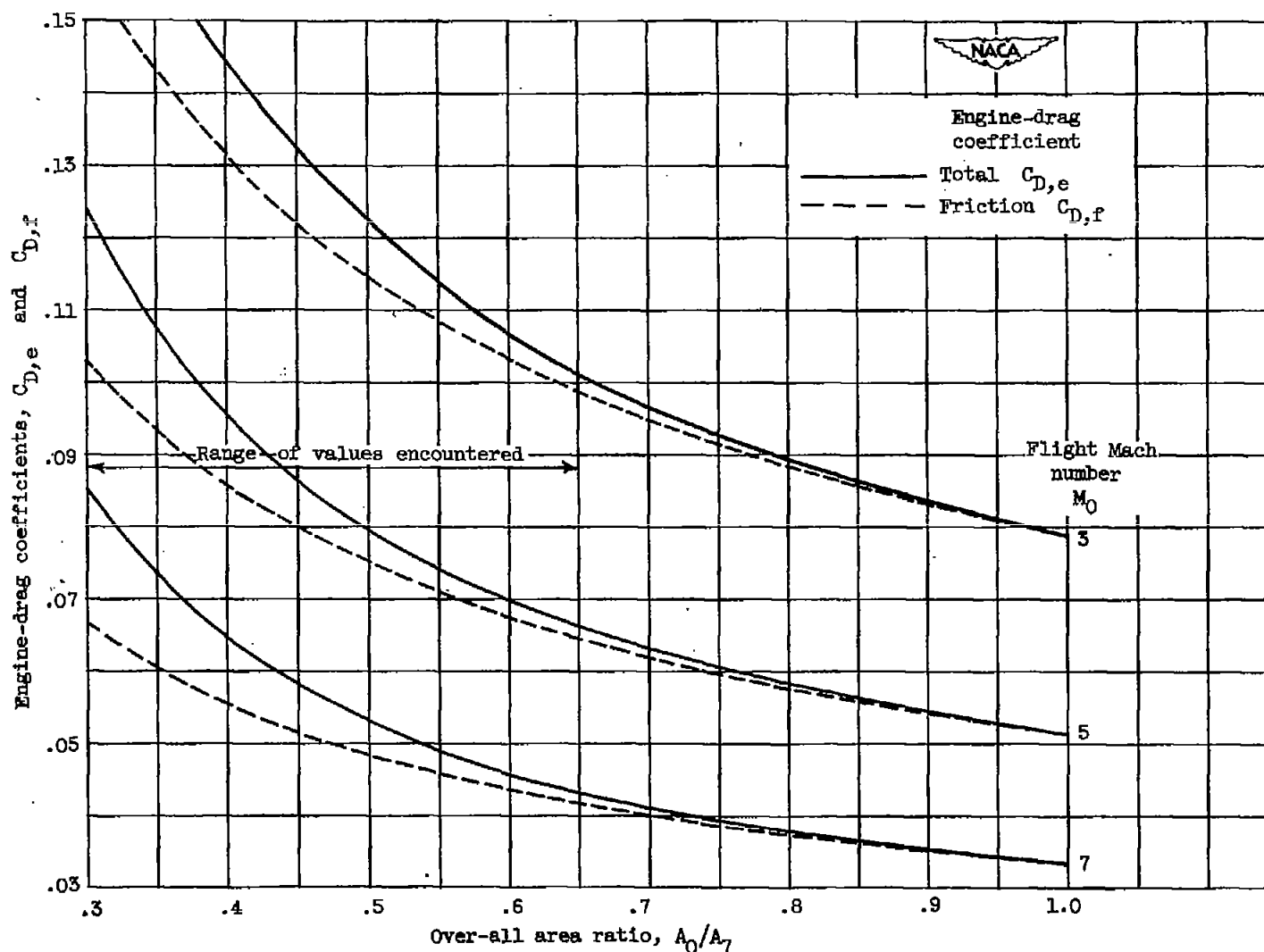


Figure 6. - Variation of external drag coefficient with over-all area ratio for various values of flight Mach number. Conical contour; length over mean diameter, 8. Coefficient based on inlet area A_0 .

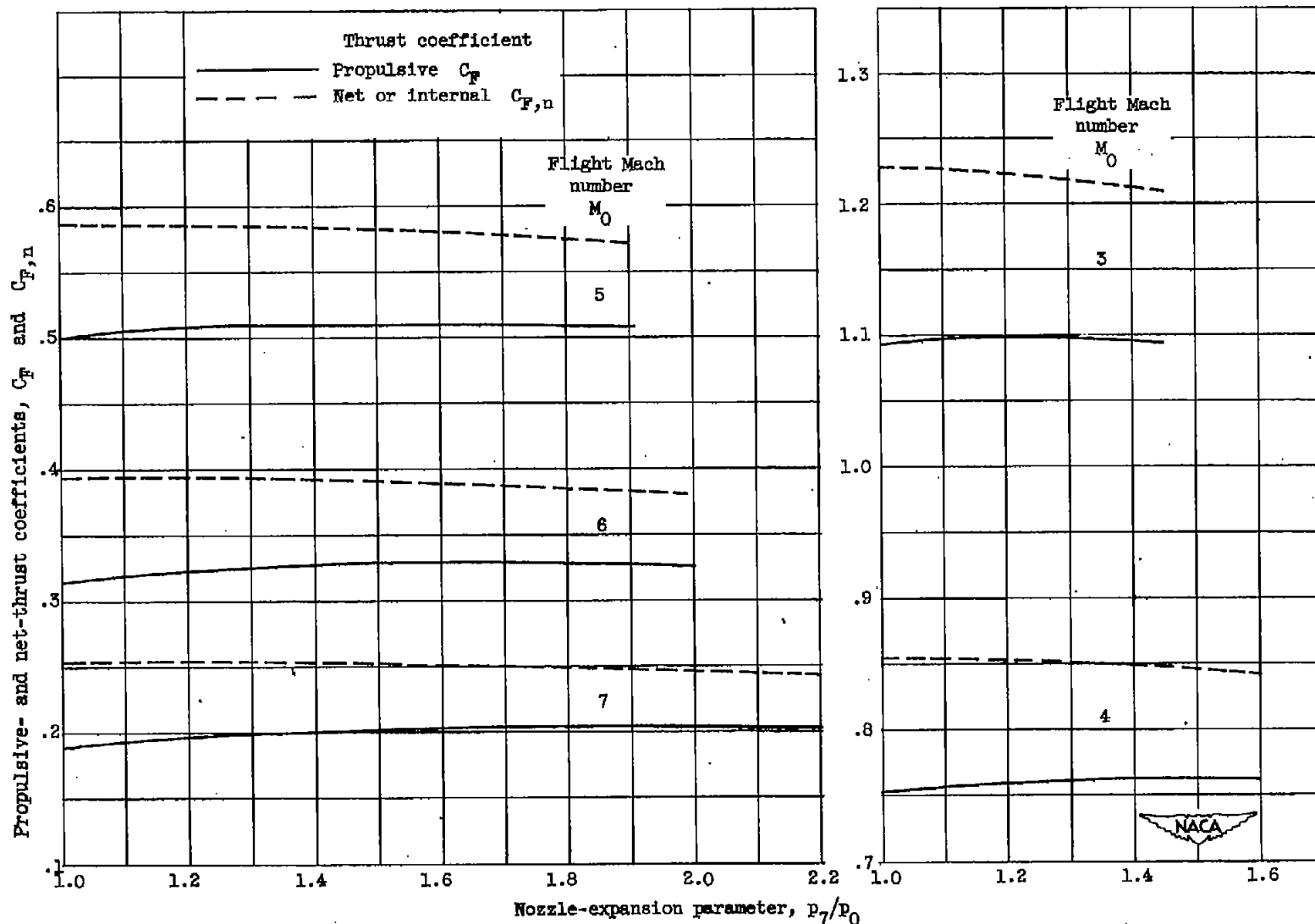


Figure 7. - Typical variations of propulsive- and net-thrust coefficients with nozzle-expansion parameter in high-efficiency engine. Energy-addition parameter, 0.4.

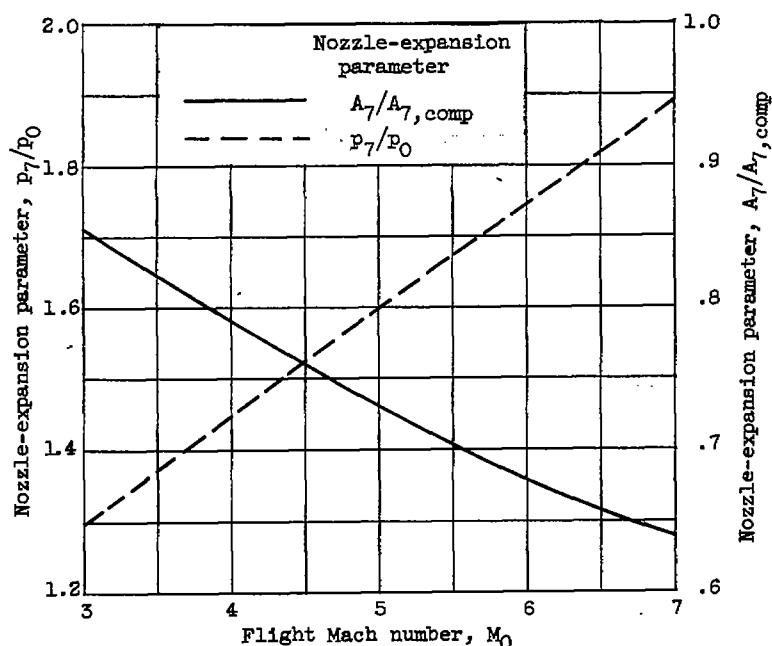


Figure 8. - Variation with flight Mach number of values of two nozzle-expansion parameters corresponding to maximum propulsive thrust at value of energy-addition parameter corresponding to maximum engine efficiency. High-efficiency engine.

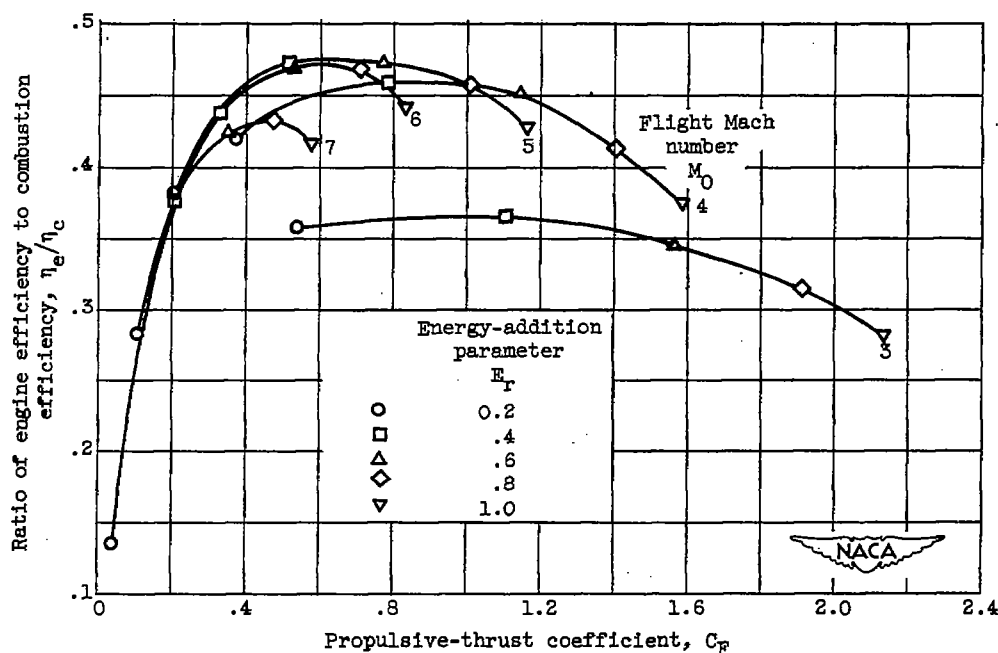


Figure 9. - Variation of ratio of engine efficiency to combustion efficiency with propulsive-thrust coefficient for various flight Mach numbers. High-efficiency engine; nozzle expansion corresponding to maximum thrust; combustor-inlet Mach number, 0.15.

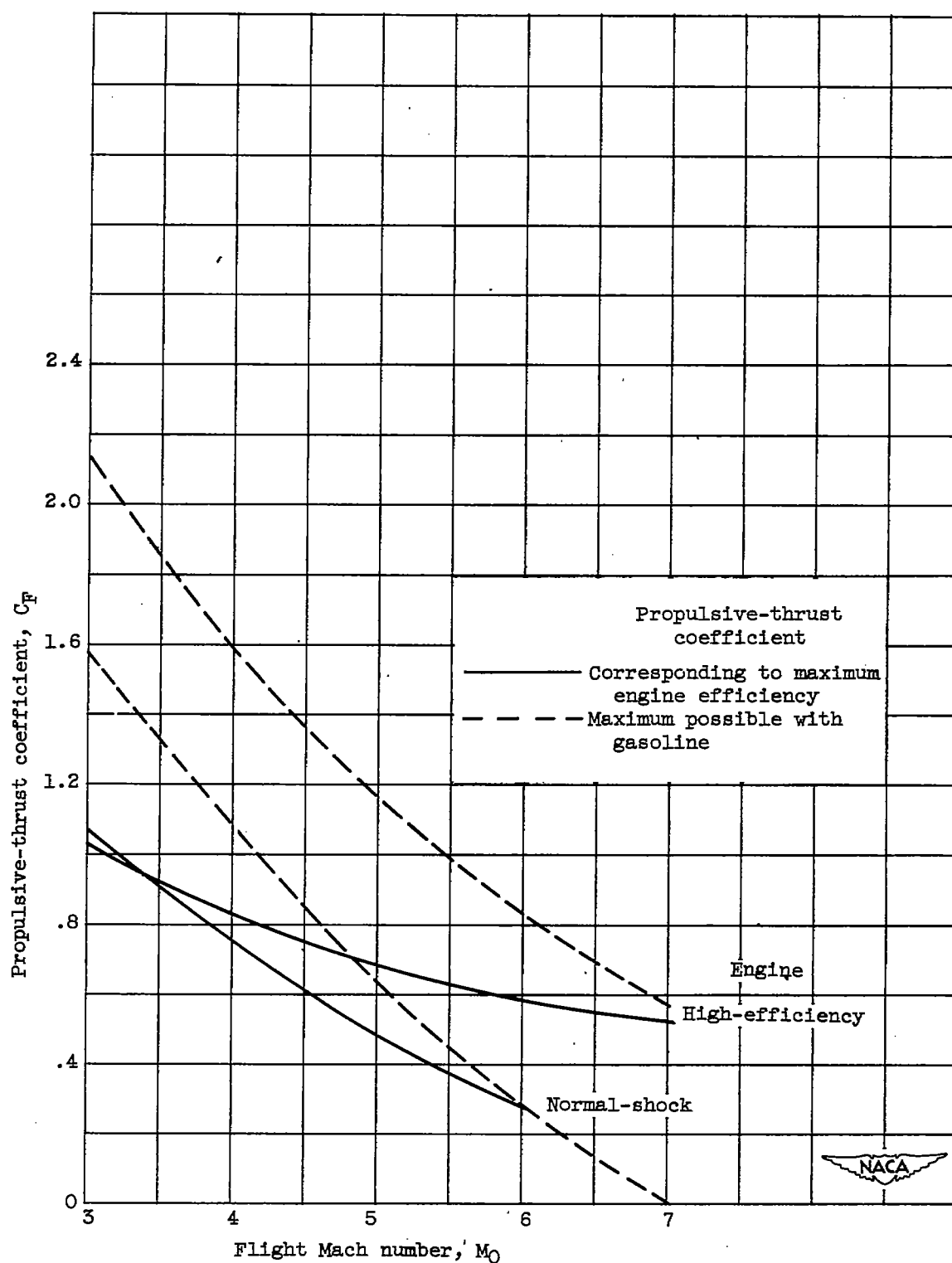


Figure 10. - Variation of propulsive-thrust coefficient with flight Mach number for two types of engine. Combustor-inlet Mach number, 0.15.

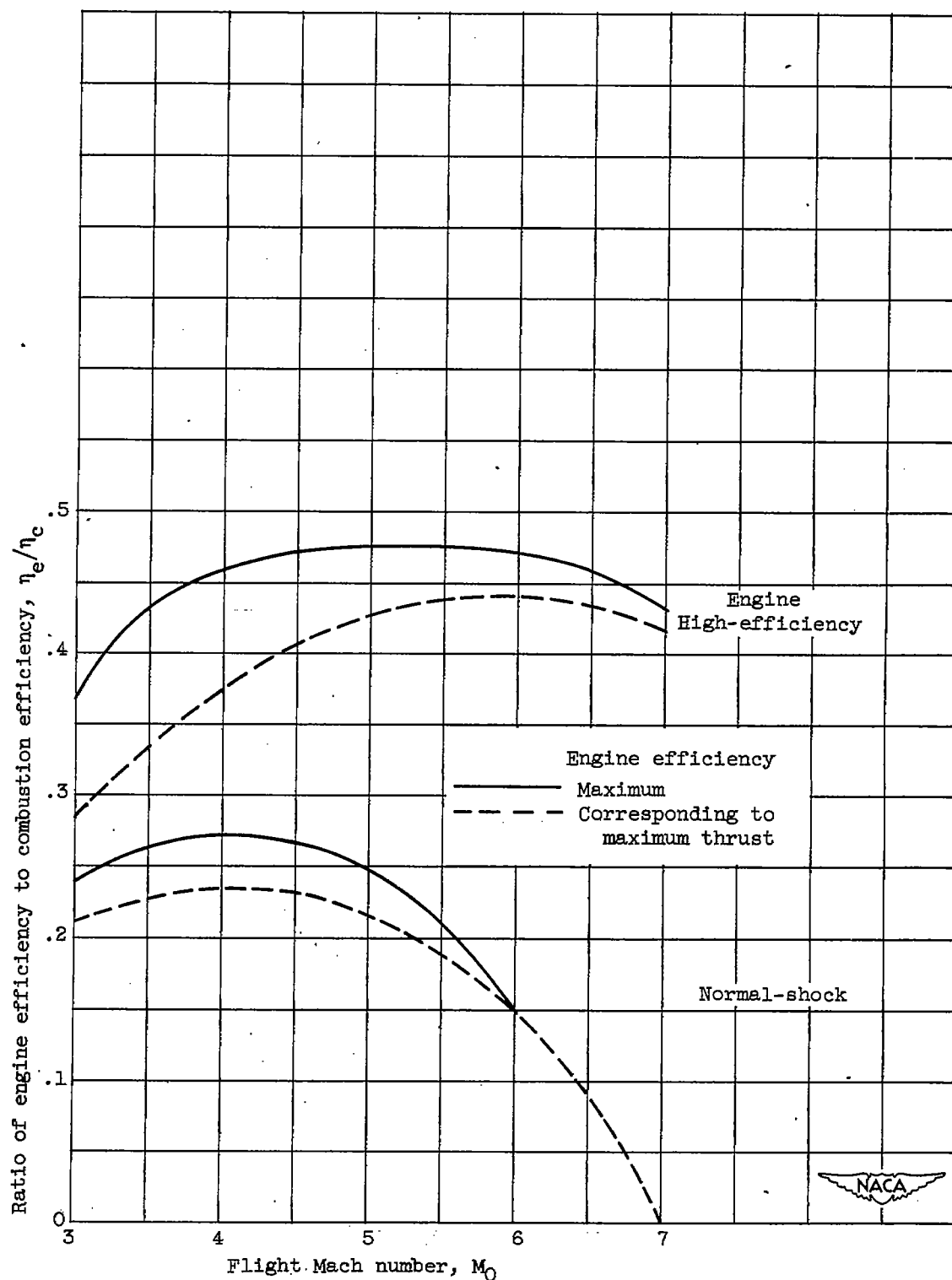
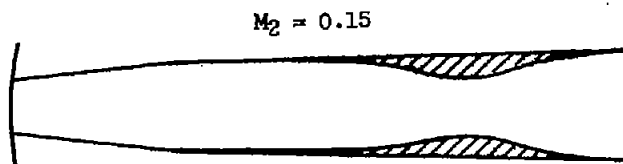
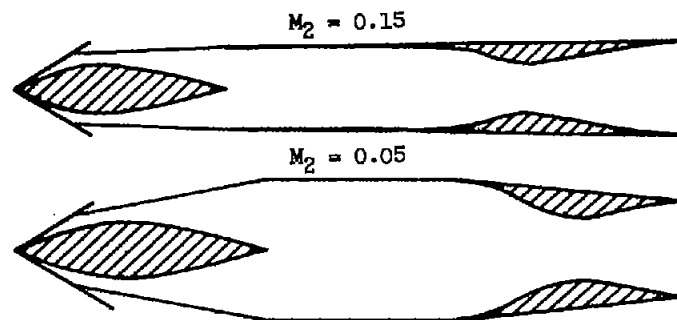


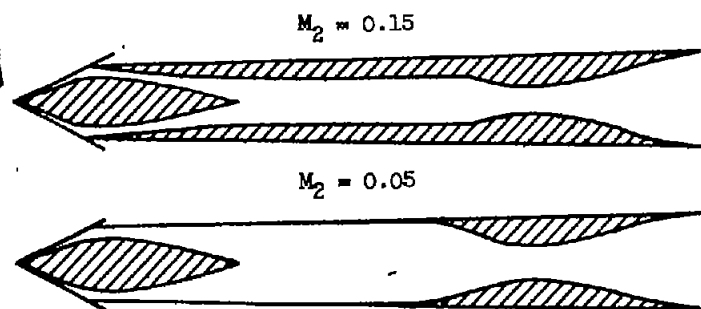
Figure 11. - Variation of ratio of engine efficiency to combustion efficiency with flight Mach number for two types of engine.



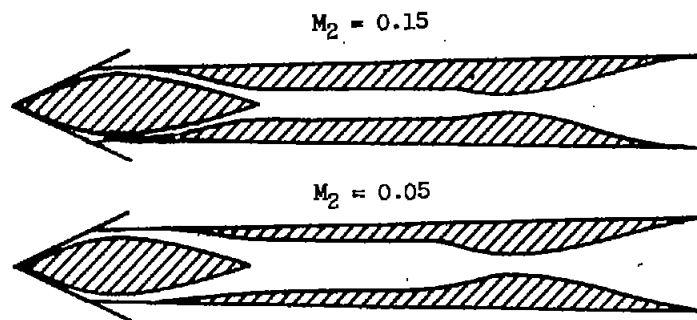
(a) Normal-shock engine; flight Mach number, 5; typical of any M_0 .



(b) High-efficiency engine; flight Mach number, 3; ratio of inlet to exit area, 0.53.



(c) High-efficiency engine; flight Mach number, 5; ratio of inlet to exit area, 0.57.



(d) High-efficiency engine; flight Mach number, 7; ratio of inlet to exit area, 0.51.

Figure 12. - Sketches showing variations of geometry with flight Mach number and combustor-inlet Mach number with areas to scale. Value of energy-addition parameter corresponds to maximum engine efficiency.